POAC'23
Glasgow, UK

Proceedings of the 27th International Conference on
Port and Ocean Engineering under Arctic Conditions
12-16 June 2023, Glasgow, UK

Prediction of Ice Resistance of an Icebreaker under Level Ice

Joon Kim[1], , Dongho Yoon[1], Seong-Yeob Jeong[2], Kwang-Jun Paik[1], Joonmo Choung[1]
[1]Inha University, Incheon, Republic of Korea
[2]Korea Research Institute of Ships and Ocean Engineering, Daejeon, Republic of Korea

ABSTRACT

Icebreakers going through level ice zone in the Arctic Sea routes are subjected to level ice-breaking loads and broken ice floe and pack ice-induced loads simultaneously; hence, it is important to estimate the ice loads on the icebreaker. This paper aims to estimate ice resistance of a model icebreaker which is towed through an ice sheet zone in a Korean arctic basin. In this study, a new approach using HydroQus, hydrodynamic subroutine for Abaqus, without Eulerian domain was introduced. The icebreaker model ship was modeled as a rigid body. HydroQus supplied non-linear hydrostatic force and hydrodynamic force in real time to the ice sheet and the broken ices separated from the level ice after the ship's ice breaking. Hydrodynamic form-induced drag forces were exerted on the level ice and the broken ices. Ice material was modeled with four node tetrahedron elements. Drucker-Prager yield function was applied to the level ice. Continuum damage mechanics model was introduced to involve ice breaking. The level icebreaking was very well simulated showing realistic breaking pattern. The broken pack ices separated from the level ice due to icebreaking were interacted with hull bottom.

KEY WORDS: Level ice; Icebreaker; Drucker-Prager yield function; Continuum damage mechanics; HydroQus.

Introduction

Global warming has increased needs for exploration of oil and gas resources; thus, Arctic shipping routes has been highlighted. Development of icebreakers with increased ice resistance is necessary. Level ice is most common condition in polar sea, so continuous level ice breaking capacity is of importance.

In addition, a simplified or formula-based approach to predict ice resistance was proposed (Lindqvist, 1989) where five parameters controls ice resistance; main dimensions, hull form, ice thickness, friction coefficient, and ice strength. He tried to explain much of energy was absorbed by crushing model prior to the bending failure. More advancement was achieved by using a numerical method based on the empirical formulas in terms of crushing pressure and bending failure of level ice (Su et al., 2010). A somewhat different approach was done by

Lubbad & Løset (2011); they established a numerical method based on some analytic equations to represent the ice breaking process, solving the equations of rigid body motions for all ice floes. They also validated their simulation results against model- and full-scale test data. A similar approach was proposed; they insisted that a more realistic breaking pattern could be observed by assuming the bending moment induced the formation of circumferential ice cracks (Huisman et al., 2016). Ko et al. (2016) modified previous study (Su et al., 2010). Namely, they suggested a varying crushing stress formula to reduce excessive crushing stress at the long parallel midship parts in commercial icebreaking ships. Jeong et al. (2017) conducted a similar approach to Lindqvist approach (1989). A focus was made that a level ice is not any more uniform but it is a naturally broken ice floe field. Two ice breaking modes were suggested: the local out-of-plane flexural failure and the global in-plane splitting failure modes (Lu et al., 2015a, 2015b). Lu et al. (2015a) introduced linear elastic fracture mechanics (LEFM) to predict global in-plane splitting failure of a large sized ice floe. Lu et al. (2016) later developed a numerical simulation code by combining two failure modes.

Finite element analysis (FEA) is understood as a very good tool for the prediction of ice resistance against some sloping structures such as icebreaker bows and lighthouse sloping plates. Two different approaches have been mainly published; first one is based on cohesive elements, the other depends on discrete elements. Lu et al. (2014) simulated ice-sloping structure interactions with the cohesive elements where the cohesive elements were separated when the displacement-based energy reached a fracture energy. A similar study was conducted by Wang et al. (2020). They generated a sheet ice field with bulk elements and cohesive elements based on Voronoi tessellations technique. Discrete elements were used to simulate sloping cone structure-sheet ice interactions (Ji et al., 2015). Compression and flexural collapse simulations made from sea ice were performed using discrete elements (Ji et al., 2017).

Somewhat different numerical techniques were conducted to predict ice resistances of ship: a meshfree method based on peridynamic model and smoothed particle hydrodynamics (SPH) method. Vazic et al. (2020) attempted to use the meshfree method to simulate global in-plane failure and out-of-plane bending failure of an ice sheet. The SPH method has led more researchers to apply it to sheet ice modeling. Zhang et al. (2019) demonstrated that the SPH could simulate three point bending failure of an ice beam, progressive accumulation of ice sheet in a simple sloping wall, and level ice breaking of an icebreaker. Ren & Park (2023) updated the SPH method and named it as moving particle semi-implicit (MPS) method. They tried to verify the MPS by simulating three point bending of an ice beam and level ice breaking of a model icebreaker.

We attempted to apply a new FEA technique to the level ice breaking simulations. The new FEA technique refers to conduct FEAs with HydroQus which is a plug-in for a commercial FEA code Abaqus. HydroQus is the acronym of hydrodynamic subroutine for Abaqus. HydroQus supports FEA by giving hydrodynamic forces at every time increment of simulation and by returning motion, velocity, and acceleration at the centre of mass of ship which are used to calculate hydrodynamic forces at next time increment. Therefore, we do not simplify or idealize the ice and ship geometries; ice thickness, ice sheet size, sloping angle of ship bow are modeled as they are expressed in their design. In addition, some important properties to determine ice resistances such as the static and kinetic friction coefficients of ice-to-ice and ice-to-hull can be simply modeled. Ice is considered as a kind of brittle materials, so the ice sheet is modeled with continuum elements. Continuum damage mechanics model is used to involve breaking of the ice elements. Towing simulation of an icebreaker model ship in a level ice condition which was conducted in a Korean ice basin. The resistances of the model ship were obtained from the towing tests with constant towing speeds. The ice resistances obtained

from as the results of the towing tests were compared with simulated results.

2. Theoretical backgrounds

2.1. Governing equation of ship motion

In line with the Newton's second law, acceleration-induced inertia force can be expressed by Equation (1) where the subscripts m and n range from 1 to 6, meaning 1 = surge, 2 = sway, 3 = heave, 4 = roll, 5 = pitch and 6 = yaw. Restoring force induced by buoyancy is proportional to the hydrostatic restoring matrix C (refer to Equation (2)).

A radiation force is comprised of the forces induced by added mass and wave damping. Two forces are linearly summed as shown in Equation(3). Added mass should be taken at very high frequency after it is stably converged so that it is no more depending on the wave excitation frequency. Meanwhile, wave damping force can be drawn by integration of impulse response function K and velocity of floating body $\dot{u}$ with respect to differential time $d\tau$. The impulse response function can be driven from wave damping coefficient B as delineated in Equation (5).

First order regular wave excitation force is given in Equation (6) that can be calculated through the real part of wave spectrum S_w and transfer function of first order wave excitation force H over k^{th} to N^{th} frequency. The superscript i is the complex number. The wave frequency should be replaced with the encounter frequency for a ship the with the forward speed. Floating structures with station keeping facilities need to consider second order wave excitation force.

The ice resistance F^{ice} between two floating bodies of icebreaker and ice sheet mainly depends on the ice sheet conditions. In this study, F^{ice} will be determined from the finite element analyses where the elastic-plastic flexibility of the ship will be considered.

$$M_{mn}\ddot{u}_m(t) = F_m^{res}(t) + F_m^{rad}(t) + F_m^{wv}(t) + F_m^{ice}(t) \quad (1)$$

$$F_m^{res}(t) = C_{mn}u_n(t) \quad (2)$$

$$F_m^{rad}(t) = m_{mn}(\infty)\ddot{u}_n(t) + \int_0^t K_{mn}(t-\tau)\dot{u}_n(\tau)d\tau \quad (3)$$

$$m_{mn}(\infty) = m_{mn}(\omega) + \int_0^\infty K_{mn}(\tau)\frac{\sin(\omega\tau)}{\omega}d\tau \quad (4)$$

$$K_{mn}(t) = \frac{2}{\pi}\int_0^\infty B_{mn}(\omega)\,cos(\omega t)\,d\omega \quad (5)$$

$$F_m^{wv}(t) = \Re\left(\sum_{k=1}^{N}\sqrt{2S_w(\omega_k)}H_m(\omega_k)e^{i(\omega_k t+\phi)}\right) \quad (6)$$

M : mass for six degrees of freedom motions

F^{res} : restoring force

u : motion component at center of mass (COM)

C : spring stiffness

F^{rad} : radiation force

m : added mass at an infinite frequency

K : impulse response function

τ : current time

B : wave damping coefficient

F^{wv} : first order wave excitation force

S_w : wave spectrum

H : first order wave excitation force RAO

ω : wave frequency or encounter frequency

ϕ : phase of first order wave excitation force RAO

2.2. Forces acting on a broken ice piece

Figure 1 depicts hydrostatic force induced by buoyancy and hydrodynamic force induced by form drag that are acting on a single broken ice piece afloat. The gravity load uniformly exerts to all ice elements, while the buoyancy force applies to the wet surface elements. Hydrostatic buoyancy force F^b acting on a broken ice piece can be determined using Equation (7) where subscript j is the identification number of a wet surface element. Equation (7) leads F^b to non-linear hydrostatic force. F^d is hydrodynamic drag force that depends on elemental drag coefficient C_d and normal component of a wet element velocity vector v_n (refer to Equation (8)). When v_n of a wet element does not direct toward sea, the drag force of the wet element vanishes zero (see Equation (9)). Due to equilibrium of gravity force and external force of $F^b + F^d$, an ice sheet and even broken ice pieces do not explode away in the simulation. For this reason, the broken pack ices floats, translates, and rotate. The motion stops when the kinetic energy is dissipated completely by the drag force.

$$F^b(t) = \rho_{sea} g \sum_{j=1} z_j A_j \tag{7}$$

$$F^d(t) = \frac{1}{2} \rho_{sea} \sum_{j=1} C_{d,j}\, v_{n,j}^2\, A_j \tag{8}$$

$$v_{n,j}(t) = \boldsymbol{n}_j \cdot \boldsymbol{v}_j \tag{9}$$

F^b : hydrostatic buoyancy force acting on a broken ice piece

g : gravitational constant

z : vertical distance from mean water level to an ice element centroid

A : area of a wet surface element of a broken ice piece

F^b : hydrodynamic drag force acting on a broken ice piece

C_d : drag coefficient of a wet surface element of a broken ice piece

v_n : projected velocity of a wet surface element of a broken ice piece

$\boldsymbol{n}$: normal vector of a wet surface element of a broken ice piece

$\boldsymbol{v}$: velocity vector of a wet surface element of a broken ice piece

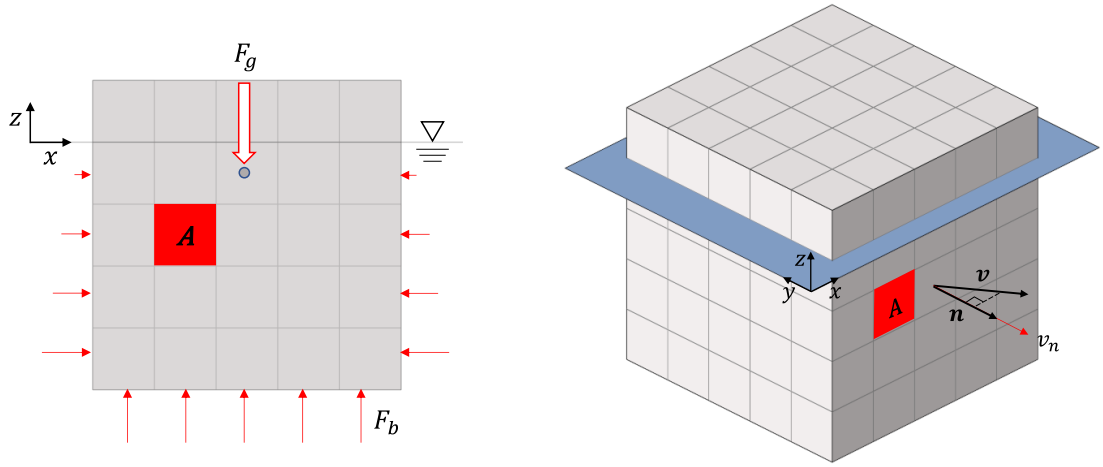

(a) buoyancy (b) drag force

Figure 1. Hydrostatic and hydrodynamic forces acting on a broken ice piece (Han et al., 2021)

2.3. Working algorithm of HydroQus

The HydroQus stands for the hydrodynamic user-subroutine for the Abaqus/Explicit (Simulia, 2023). It was developed using compiler Fortran and could be plugged into the Abaqus on every execution. The HydroQus calculates hydrodynamic loads using displacements, velocities, and accelerations at pre-selected nodes taken from Abaqus kernel at every requested time increment and feedbacks the updated hydrodynamic loads to the Abaqus for the next time increment. The hydrodynamic loads include linear or nonlinear restoring forces, linear radiation forces, and 1st and 2nd order wave excitation forces. The hydrostatic constants of linear restoring stiffnesses and hydrodynamic constants of added masses, wave damping coefficients, and wave excitation forces should be imported from results of hydrodynamic frequency response analyses using some external codes such as Aqwa (Ansys, 2022).

The HydroQus requests nodal displacements, velocities, and accelerations at user-specified nodes at every time step. Before generating time-domain hydrodynamic forces, the HydroQus reads the user-defined job file which includes restoring stiffnesses, added masses (optional), radiation damping coefficients (optional), 1st and 2nd wave excitation forces (optional), fluid density, gravitational acceleration, etc. Properties of regular or irregular wave can be alternatively assigned; for instance, wave period/wave height/incident angle, and ramp time are necessary to define a regular wave, while wave period and height are replaced with the wave spectrum parameters of wave peak period ω_p and significant wave height H_s.

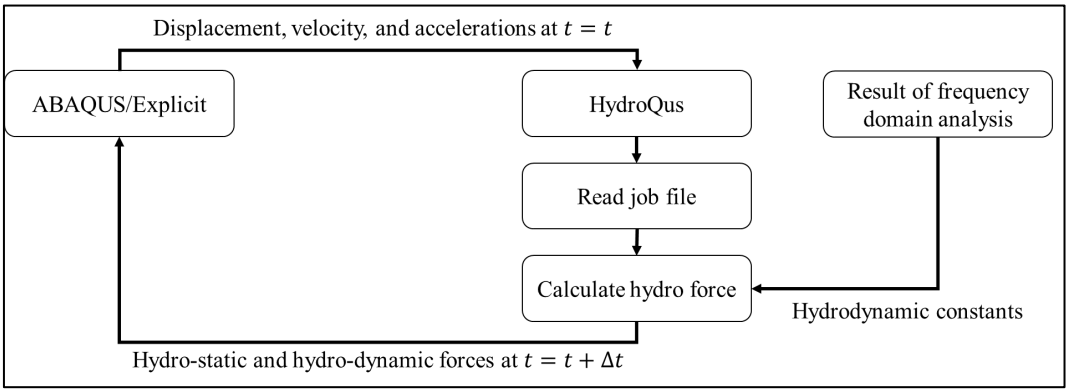

Figure 2. Working algorithm of HydroQus (Han et al., 2021)

2. Towing test simulations of a model ship

2.1. Modeling for towing simulations

The model tests were conducted in the KRISO arctic basin for the Korean research icebreaker ARAON (see Figure 3). Because the overall length of the real ship was 111m, the overall length of the model ship was 5.946m considering scale factor of 18.667 as seen in Table 1.

Table 1. Towing test conditions

Item	Value
Model ship dimensions L_{OA}×B×D (m)	5.946×1.017×0.530
Ice channel width (m)	4.0
Ice channel length (m)	32.0
Ice thickness (mm)	30.7
Density of ice (kg/m^3)	870.0
Density of basin water (kg/m^3)	1025.0
Towing speed (m/s)	0.595

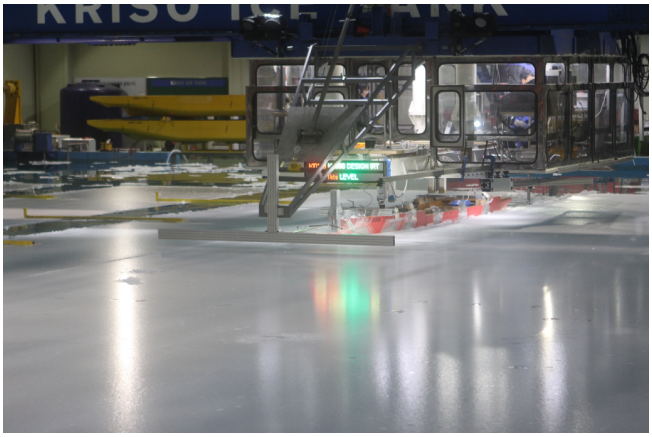

Figure 3. Towed model ship in KRISO

Altair/HyperMesh (Altair, 2022) was used to generate the model ship and ice sheet. Objective of the towing simulation is to compare the simulated ice resistance with the experimental one, thus quadrilateral and triangular rigid elements of R3D4 and R3D3 were used to construct model ship as depicted in Figure 4. A mass element (MASS) and a second moment of mass element (ROTARYI) were located at the centre of mass (COM). The model ship was fully fixed with the towing vehicle; hence the rigid model ship was constrained in sway, heave, roll, pitch, and yaw directions. Towing by the carriage vehicle was realized by applying the prescribed displacement history at the COM obtained from the towing test.

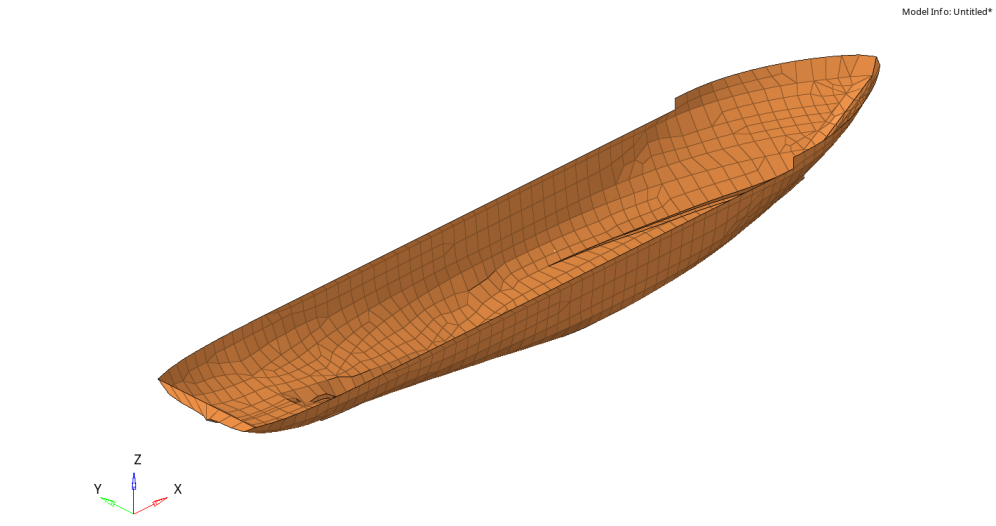

(a) isometric view

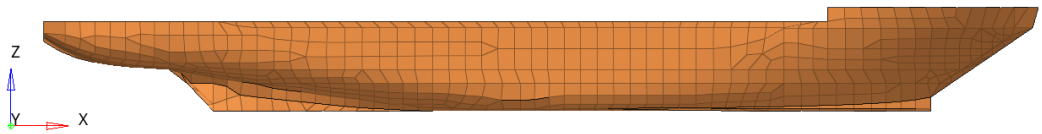

(b) side view

Figure 4. FE model of model ship

Ice sheet was modeled as tetrahedron elements of C3D4 as seen in Figure 5. The element size was determined to be 60mm considering total number of ice elements. Symmetric boundary conditions were assigned along the ice sheet borders as seen Figure 5(b). HydroQus continuously provided hydrostatic and hydrodynamic forces for the ice sheet, so the ice sheet remained afloat even without Eulerian domain.

Drucker-Prager yield potential was used to describe plastic behavior after yielding. Drucker-Prager model has been used for brittle materials of concretes, rocks, glasses, and ices. Equation (10) is Drucker-Prager yield function that is dependent on von Mises equivalent stress, Hydrostatic stress, friction angle, and cohesion strength. The cohesion strength is a function of uniaxial compressive strength and friction angle; hence the uniaxial compressive strength and friction angle remain user input. Fish & Zaretsky (1997) predicted the friction angles of ice as a function of ambient temperature. It ranges from 3º at 0 ℃ to 8º at -20 ℃. We assumed the friction angle was 20º in this simulation.

$$S = \sigma_v + \sigma_h \tan\beta + d \quad (10)$$

S : Yield surface

σ_v : von Mises equivalent stress

σ_h : hydrostatic stress

β : friction angle

d : cohesion strength

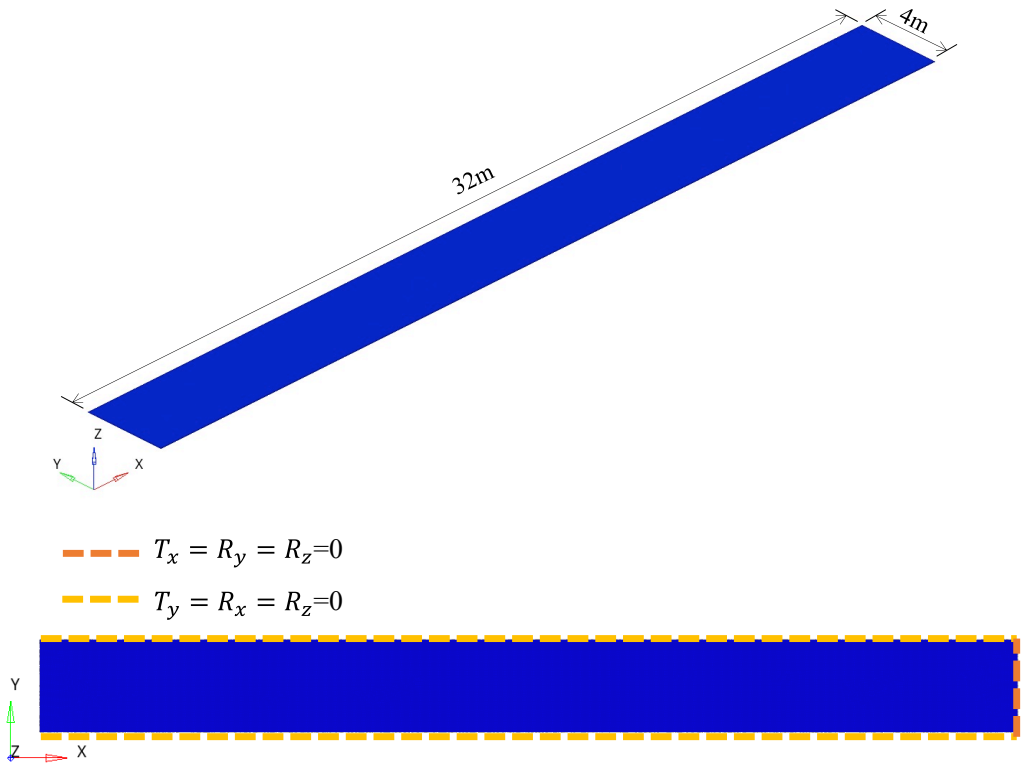

Figure 5. FE model of ice sheet

Table 2. Towing simulation properties

Item	Value
Elastic modulus of ice (MPa)	100.0
Poisson ratio of ice	0.3
Uniaxial compressive yield strength of ice (MPa)	0.12
Friction angle of ice (degree)	20.0
Damage initiation strain	0.006
Fracture energy (N/m)	44.2
Friction coefficient between ice and ship	0.05
Friction coefficient between ices	n/a

The elastic modulus, Poisson ratio, uniaxial compressive yield strength, friction coefficient of ice listed in Table 2 were provided by KRISO. Some studies have introduced a concept of

continuum damage mechanics (CDM) to realize erosion of elements in the ice breaking simulations (Han et al., 2017; Jeon & Kim, 2021). CDM uses associated flow rule and thus flow stress should vary with damage status. Flow stress degradation starts at damage initiation strain and material stiffness loses completely when nominal displacement or nominal energy in an element reaches a predefined criterion.

We assumed that damage initiation strain was five times of the uniaxial compressive yield strain. Meanwhile, the nominal strain at fracture compression force (fracture strain) was two times of the damage initiation strain. Finally, the fracture energy of 44.2 N/m could be easily determined with the fracture strain and ice thickness.

2.2. Results for towing simulations

Objective of this section is to view if the FEA-based simulation well predicts the ice resistance of the model ship. Figure 6 depicts time versus towing resistance curves obtained from the test and simulation. We applied the test towing speed to the simulation. Even though the sampling rate was 0.01s both in the test and simulation, data fluctuation in the simulation is severer then in the test. For the quantified comparison of the ice resistance, we averaged the towing resistance for stably uniform towing interval of 25s-45s. Test average was 163.4N, while simulated one was 165.4N. Therefore we can conclude that a very reliable simulation was conducted with suitable simulation condition.

Ice breaking patterns at t=25s and t=45s were presented in Figure 7. The ice breaking pattern was similar to that during the towing test in which a global splitting pattern has been reported. The ice floes and pack ices after ice breaking did not fly away or sink down because HydroQus provided hydrostatic and hydrodynamic forces in real time.

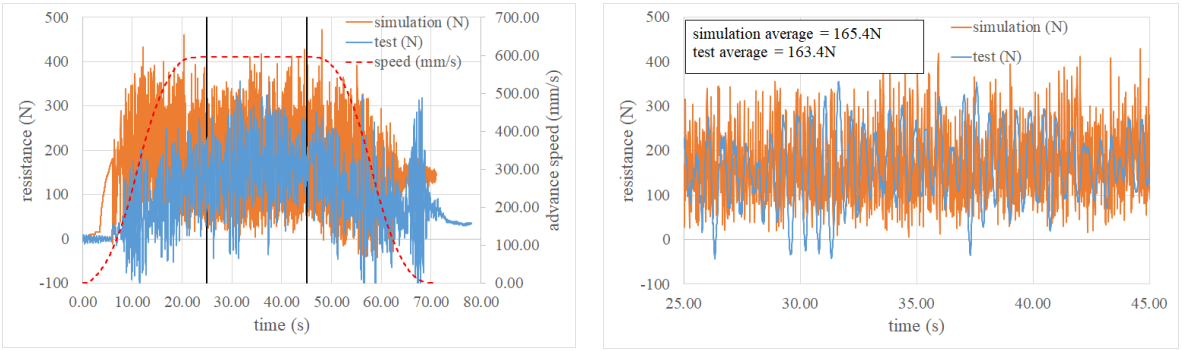

(a) entire towing range (b) effective towing range

Figure 6. Time resistance curves

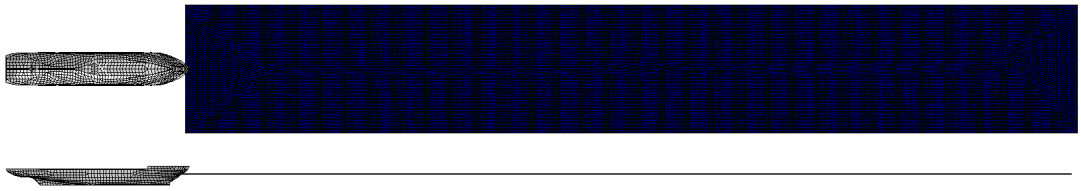

(a) t = 0s

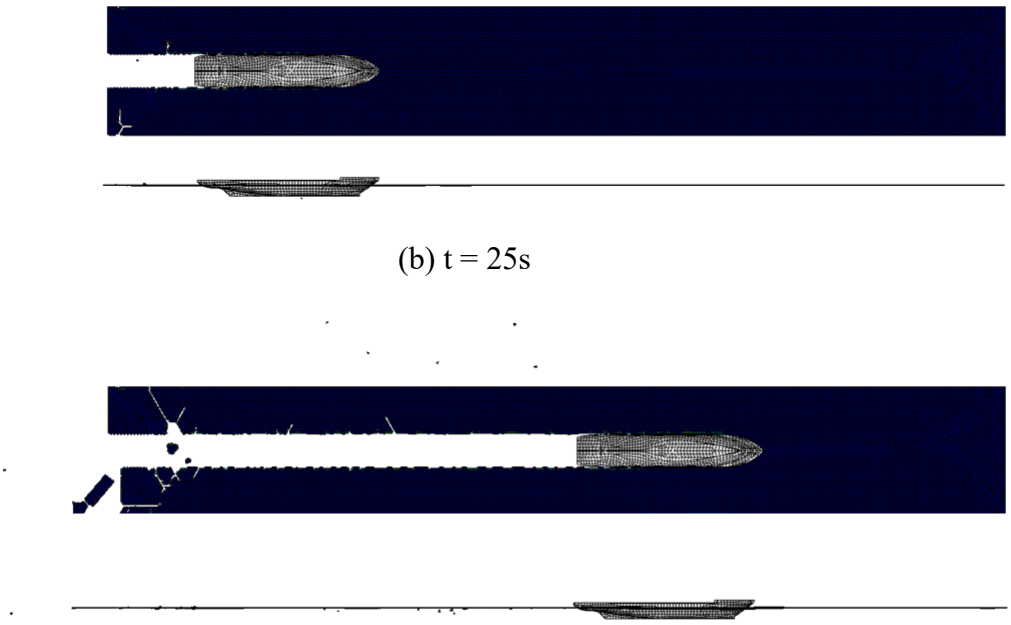

(b) t = 25s

(c) t=45s

Figure 7. Icebreaking pattern during towing simulation

4. Conclusions

Icebreakers going through level ice zone in the Arctic Sea routes are subjected to level ice-breaking loads and ice floe loads after ice breaking; hence, it is important to estimate the ice loads on the icebreaker. In this study, a new approach without the Eulerian domain, HydroQus was introduced to produce and provide hydrostatic and hydrodynamic loads to ice sheet, ice floes, and pack ices. This paper used the model ship of an icebreaker. The icebreaker was modeled as a rigid body with assumed mass information. The level ice and broken ices such as ice floes and pack ices were under hydrostatic non-linear restoring forces and hydrodynamic form-induced drag forces.

Ice material was modeled with four node tetrahedron elements. Drucker-Prager yield function was applied to the level ice. Energy-based damage model was used to induce level ice breaking. The level icebreaking was very well simulated showing global splitting failure and local bending failure. The broken ice floes were interacted with hull bottom and ice sheet.

Level ice breaking simulations of real icebreaker will be conducted. The hydrodynamic radiation effects will be included in the simulations. In addition, ice breaking patterns will be monitored.

FUNDING

This work was supported by Korea Environmental Industry & Technology Institute (KEITI) funded by Korea Ministry of Environment (No. 146836), Korea Energy Technology Evaluation and Planning (KETEP) funded by the Ministry of Trade, Industry and Energy of

Korea (No. 20213000000030), and Korea Institute of Marine Science and Technology Promotion (KIMST) funded by the Ministry of Oceans and Fisheries (No. 202202103).

REFERENCES

Altair. (2022). *HyperWorks User Manual*. Altair.

Ansys. (2022). *Ansys User Manual*. Ansys.

Fish, A. M., & Zaretsky, Y. K. (1997). *Ice Strength as a Function of Hydrostatic Pressure and Temperature.* (CRREL Report 97-6; p. 14). Cold Regions Research & Engineering Laboratory, US Army Corps of Engineers. https://usace.contentdm.oclc.org/digital/api/collection/p266001coll1/id/6095/download

Han, D., Lee, H., Choung, J., Kim, H., & Daley, C. (2017). Cone ice crushing tests and simulations associated with various yield and fracture criteria. *Ships and Offshore Structures*, *12*(sup1), S88–S99. https://doi.org/10.1080/17445302.2016.1266920

Han, D., Paik, K.-J., Jeong, S.-Y., & Choung, J. (2021). Prediction of the ice resistance of icebreakers using explicit finite element analyses with a real-time load control technique. *Ocean Engineering*, *240*, 109825. https://doi.org/10.1016/j.oceaneng.2021.109825

Huisman, M., Janßen, C. F., Rung, T., & Ehlers, S. (2016). Numerical Simulation of Ship-Ice Interactions with Physics Engines under Consideration of Ice Breaking. *The Proceedings of The Twenty-Sixth (2016) International OFFSHORE AND POLAR ENGINEERING CONFERENCE*, 1174–1180.

Jeon, S., & Kim, Y. (2021). Numerical simulation of level ice–structure interaction using damage-based erosion model. *Ocean Engineering*, *220*, 108485. https://doi.org/10.1016/j.oceaneng.2020.108485

Jeong, S.-Y., Choi, K., Kang, K.-J., & Ha, J.-S. (2017). Prediction of ship resistance in level ice based on empirical approach. *International Journal of Naval Architecture and Ocean Engineering*, *9*(6), 613–623. https://doi.org/10.1016/j.ijnaoe.2017.03.007

Ji, S., Di, S., & Liu, S. (2015). Analysis of ice load on conical structure with discrete element method. *Engineering Computations*, *32*(4), 1121–1134. https://doi.org/10.1108/EC-04-2014-0090

Ji, S., Di, S., & Long, X. (2017). DEM Simulation of Uniaxial Compressive and Flexural Strength of Sea Ice: Parametric Study. *Journal of Engineering Mechanics*, *143*(1), C4016010. https://doi.org/10.1061/(ASCE)EM.1943-7889.0000996

Ko, D., Park, K.-D., & Ahn, K. (2016). Time domain simulation for icebreaking and turning capability of bow-first icebreaking models in level ice. *International Journal of Naval Architecture and Ocean Engineering*, *8*(3), 228–234.

https://doi.org/10.1016/j.ijnaoe.2016.02.004

Lindqvist, G. (1989). A Straightforward Method for Calculation of Ice Resistance of Ships. *The Proceedings of 10th International Conference on Port and Ocean Engineering under Arctic Conditions*, 722–735.

Lu, W., Lubbad, R., & Løset, S. (2014). Simulating Ice-Sloping Structure Interactions With the Cohesive Element Method. *Journal of Offshore Mechanics and Arctic Engineering*, *136*(3), 031501. https://doi.org/10.1115/1.4026959

Lu, W., Lubbad, R., & Løset, S. (2015a). In-plane fracture of an ice floe: A theoretical study on the splitting failure mode. *Cold Regions Science and Technology*, *110*, 77–101. https://doi.org/10.1016/j.coldregions.2014.11.007

Lu, W., Lubbad, R., & Løset, S. (2015b). Out-of-plane failure of an ice floe: Radial-crack-initiation-controlled fracture. *Cold Regions Science and Technology*, *119*, 183–203. https://doi.org/10.1016/j.coldregions.2015.08.009

Lu, W., Lubbad, R., Løset, S., & Kashafutdinov, M. (2016). Fracture of an ice floe: Local out-of-plane flexural failures versus global in-plane splitting failure. *Cold Regions Science and Technology*, *123*, 1–13. https://doi.org/10.1016/j.coldregions.2015.11.010

Lubbad, R., & Løset, S. (2011). A numerical model for real-time simulation of ship–ice interaction. *Cold Regions Science and Technology*, *65*(2), 111–127. https://doi.org/10.1016/j.coldregions.2010.09.004

Ren, D., & Park, J.-C. (2023). Particle-based numerical simulation of continuous ice-breaking process by an icebreaker. *Ocean Engineering*, *270*, 113478. https://doi.org/10.1016/j.oceaneng.2022.113478

Simulia. (2023). *Abaqus—SIMULIA User Assistance 2023*. https://help.3ds.com/2023/English/DSSIMULIA_Established/SIMULIA_Established_FrontmatterMap/sim-r-DSDocAbaqus.htm?contextscope=all

Su, B., Riska, K., & Moan, T. (2010). A numerical method for the prediction of ship performance in level ice. *Cold Regions Science and Technology*, *60*(3), 177–188. https://doi.org/10.1016/j.coldregions.2009.11.006

Vazic, B., Oterkus, E., & Oterkus, S. (2020). In-Plane and Out-of Plane Failure of an Ice Sheet using Peridynamics. *Journal of Mechanics*, *36*(2), 265–271. https://doi.org/10.1017/jmech.2019.65

Wang, Y., Yao, X., Teo, F. C., & Zhang, J. (2020). Cohesive Element Method to Level Ice-sloping Structure Interactions. *International Journal of Offshore and Polar Engineering*, *30*(4), 385–394. https://doi.org/10.17736/ijope.2020.jc787

Zhang, N., Zheng, X., Ma, Q., & Hu, Z. (2019). A numerical study on ice failure process and

ice-ship interactions by Smoothed Particle Hydrodynamics. *International Journal of Naval Architecture and Ocean Engineering*, *11*(2), 796–808. https://doi.org/10.1016/j.ijnaoe.2019.02.008